

## Supplementary Online Content

Morris LGT, Chandramohan R, West L, et al. The molecular landscape of recurrent and metastatic head and neck cancers: insights from a precision oncology sequencing platform. *JAMA Oncol*. Published online July 21, 2016. doi:10.1001/jamaoncol.2016.1790

**eAppendix.**  
**Supplement 2 Table Legends.**  
**eReferences.**  
**eFigures 1-19.**

This supplementary material has been provided by the authors to give readers additional information about their work.

## eAppendix

### SUPPLEMENTARY METHODS

#### Patients and tumor samples

The MSK-IMPACT (Memorial Sloan Kettering – Integrated Mutation Profiling of Actionable Cancer Targets) assay is a next-generation sequencing (NGS) assay approved for clinical use through CLIA (Clinical Laboratory Improvement Amendments) by the Centers for Medicare and Medicaid Services<sup>1</sup>. The majority of patients have recurrent or metastatic disease but patients are otherwise unselected. Since 2014, over 9,000 solid tumors have been profiled using MSK-IMPACT.

We reviewed all patients treated by the MSK multidisciplinary head and neck oncology team, whose tumors were sequenced with MSK-IMPACT in the context of an Institutional Review Board (IRB)-approved study (NCT01775072). Of 224 patients enrolled, 151 with a minimum of 6 month clinical followup, whose tumors were sequenced between January 2014 and July 2015, were included. This analysis was approved by the MSK IRB. Correlative clinical data are recorded prospectively in an IRB-approved database. Human papillomavirus (HPV) status was determined by p16 immunohistochemistry and HPV in situ hybridization as part of routine care. Treatment(s) initiated after ordering NGS were considered to be guided by molecular data if results led to, or justified continuation with, a specific treatment.

#### Sequencing platform and variant calling

MSK-IMPACT is optimized for DNA extracted from low-input formalin-fixed, paraffin embedded (FFPE) samples. The assay is designed to detect single nucleotide variants (SNVs), indels, copy number variants (CNVs) and structural variants in genes that are functionally relevant to cancer and/or clinically actionable targets. The current assay uses hybrid capture technology (Nimblegen SeqCap EZ library custom oligo) to perform deep (>200x) sequencing (Illumina HiSeq 2500) of all 5781 exons and selected introns of 410 cancer genes, including canonical and selected non-canonical transcripts, the *TERT* promoter region, and 33 introns of 14 rearranged genes (**eTable 1**). The panel includes 1042 tiling probes covering single nucleotide polymorphisms (SNPs), allowing genotyping to ensure tumor-normal matching, identify contaminating DNA, and serve as a low-density SNP array for CNV analysis. MSK-IMPACT has been extensively validated. Specific details of panel design, capture protocol, sequencing, quality control, read alignment, and variant calling have been described<sup>2,3</sup>. Molecular alterations were classified according to MSK levels of evidence that support standard or investigational therapeutic indications (**eTable 2**).

#### Bioinformatic analyses

Additional copy number analyses were performed using FACETS<sup>4</sup>, which performs segmentation of total and allelic copy ratio, and estimates allele-specific copy number, in targeted capture sequencing data. We used FACETS to identify whole genome duplication (WGD) and deletion of 3p in SCC (**eFigures 1-2**).

The fraction of the genome with copy number alteration was defined with a  $\log_2$  copy number ratio threshold of .2 or -.2. For comparison, tumor ploidy and allele-specific copy number in The Cancer Genome Atlas (TCGA) HNSCC cases<sup>5</sup> were determined using SNP6 copy number data input into ASCAT<sup>6</sup>, as previously described<sup>7</sup>.

Analyses of intratumor heterogeneity were also performed using FACETS, which estimates the cancer cell fraction of somatic variants, by incorporating variant allelic fraction and adjusting for tumor purity and underlying copy number<sup>4</sup>. The cancer cell fractions of somatic variants are expressed with intervals representing full width at half maximum boundaries. Mutations with an upper boundary overlapping 1.0 were considered clonal; those with an upper boundary <0.95 were considered to be subclonal, similar to the approach described by McGranahan et al<sup>8</sup>. Mutations with overlapping confidence intervals were considered to comprise an individual subclonal or clonal population, and the total number of subclonal populations, SNVs, and subclonal SNVs was determined for each sample. These parameters were compared among subsets using stepwise logistic regression to control for HPV status, site sequenced, purity, and ploidy.

Network analyses of SNVs were performed in Cytoscape 3.2.1 using CyniTools to infer significant positive and negative correlations<sup>9</sup>. Functional annotations were analyzed by examining enrichment of Gene Ontology terms with BINGO<sup>10</sup>.

Nonsynonymous and synonymous SNVs were used to delineate certain mutational signatures. The APOBEC enrichment score, previously described, represents the enrichment of mutated C (or G) within TCW (or WGA) motifs, in context of all mutated C (or G) 20 nucleotides upstream/downstream<sup>11</sup>. For the tobacco signature, the number of transversions per tumor was calculated. The UV signature was based on a predominance of C to T (or G to A) transitions in dipyrimidine contexts<sup>12</sup>.

Somatic alteration profiles of HNSCC were examined using a binary classifier to determine if profiles most closely resembled HPV-positive or HPV-negative tumors. A support vector machine (SVM) algorithm (in GenePattern<sup>13</sup>) maximizes the hyperplane separating HPV-positive and HPV-negative samples<sup>14</sup>. The SVM model was first trained and cross-validated in the TCGA cohort of 298 cases with somatic alteration (mutations and high-level CNVs in MSK-IMPACT genes) and HPV status information. The model had 88% accuracy ( $p < 10^{-6}$ ) in the validation set. The model was then applied to MSK-IMPACT samples, and HPV status predicted for each case. A posterior probability ("confidence") for each sample classification represents distance from the hyperplane.

To determine if certain frequent genetic alterations were more common than expected in recurrent/metastatic tumors, the MSK-IMPACT and TCGA cohorts were compared using enrichment analysis. To allow for potential differences in sequencing platforms, enrichment was calculated as the log-ratio of odds ratios: the odds ratio (OR) for alterations occurring in HPV-negative tumors, compared to HPV-positive tumors, was calculated within each cohort, and ORs compared between cohorts. Significance was tested with logistic regression using an interaction term:

$$\text{logit (probability of variant)} = \beta_0 + \beta_1(\text{cohort}) + \beta_2(\text{HPV status}) + \beta_3 (\text{cohort} \times \text{HPV status})$$

Where  $e^{\beta^3}$  is the enrichment for an alteration in MSK-IMPACT HPV-positive tumors, compared to TCGA tumors.

### **Germline variant analysis**

After IRB approval for additional germline analyses, these were performed as previously described<sup>3</sup>. Briefly, SNVs and indels identified in anonymized normal DNA were analyzed in Ingenuity Variant Analysis software, categorizing variants by pathogenicity based on 2015 ACMG guidelines<sup>15</sup>. Pathogenic and likely pathogenic variants were manually confirmed. We also included 93 genes in Online Mendelian Inheritance in Man (OMIM) that have been associated with susceptibility to any cancer type<sup>3</sup>, and 26 genes recommended by the ACMG<sup>16</sup>.

## SUPPLEMENT 2 TABLE LEGENDS

**eTable 1.** List of 410 genes (entire exonic regions included) and 36 additional intronic regions included in the MSK-IMPACT next-generation sequencing panel.

**eTable 2.** Actionable molecular alterations, categorized by MSK levels of evidence.

**eTable 3.** Clinical and tumor characteristics of 151 patients with recurrent/metastatic and treatment-resistant head and neck cancers. HNSCC, head and neck squamous cell carcinoma. ACC, adenoid cystic carcinoma. NPC, nasopharyngeal carcinoma. ONB, olfactory neuroblastoma. CT, chemotherapy. RT, radiation therapy.

**eTable 4.** Matrix of clinical data and genetic alterations found in 151 advanced head and neck cancers, subdivided by cancer type. Each alteration is described as: mutation genomic coordinates, nucleotide variant, amino acid variant, variant allelic frequency, category of mutation | copy number alteration.

**eTable 5.** Gene ontology annotations enriched in the cluster of genes more frequently altered in HPV-positive HNSCC (clusters of green nodes in Figure 2D), with statistical testing corrected using Benjamini-Hochberg false discovery rate.

**eTable 6.** FACETS estimates of tumor purity, ploidy, number of subclonal populations and number of subclonal mutations (see Methods) for HNSCC cases.

**eTable 7.** Multivariable logistic regression models of the associations between intratumor heterogeneity and (A) HPV status and (B) tumor site (primary vs. recurrence/metastasis); (C) (sub)clonal status of TP53 mutations in HPV-positive and HPV-negative HNSCC samples.

**eTable 8.** Odds ratios for common somatic alterations in HPV-negative compared to HPV-positive tumors, in both recurrent/metastatic (MSK-IMPACT) and primary (TCGA) HNSCC datasets. Enrichment is calculated as the ratio of odds ratios. Significance testing as indicated.

**eTable 9.** TP53 mutations in 16 recurrent/metastatic HPV-associated cervical carcinoma sequenced on MSK-IMPACT.

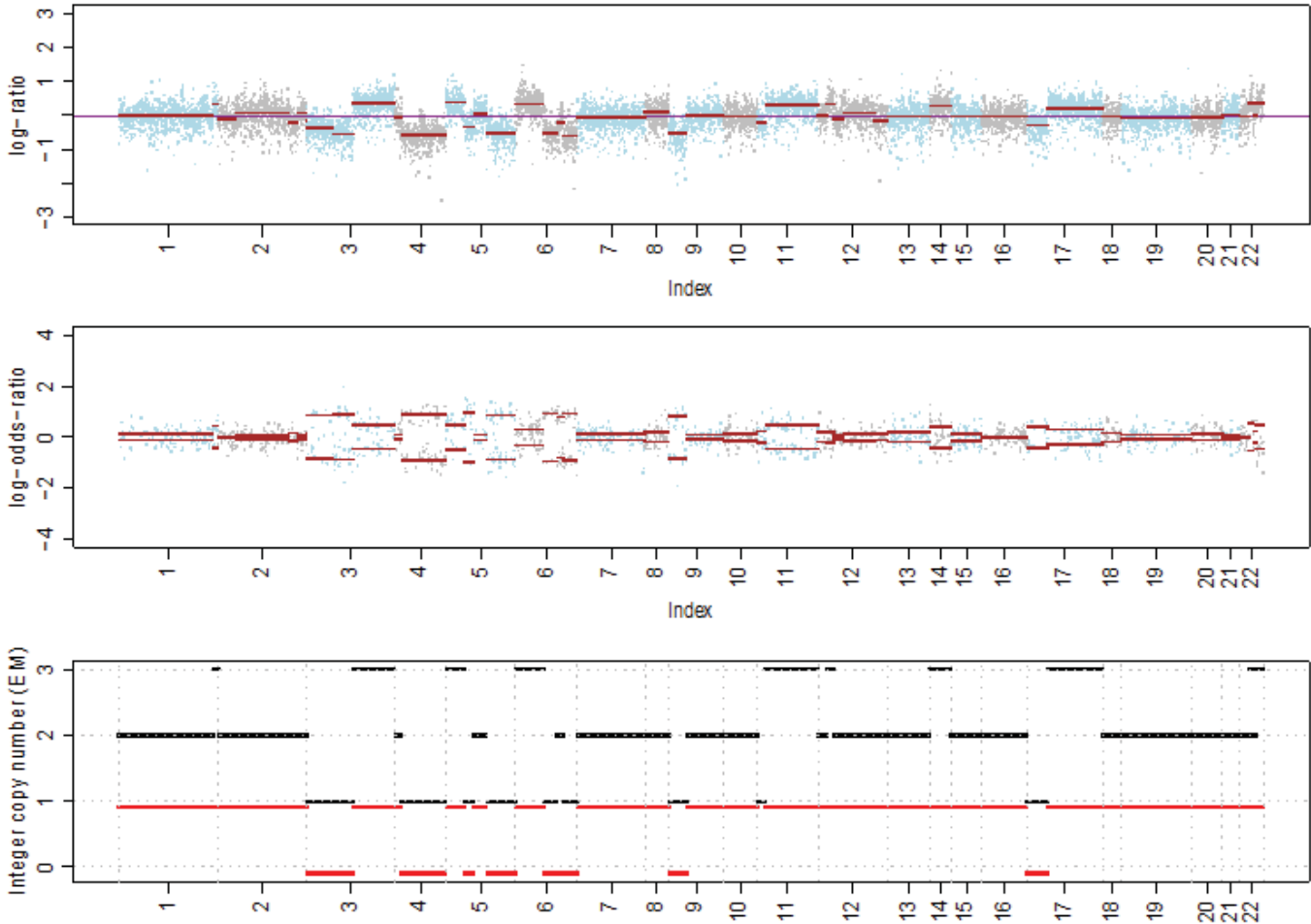
**eTable 10.** REMARK (Reporting recommendations for tumor marker studies) checklist.

## REFERENCES (For Supplementary Methods)

1. Hyman DM, Solit DB, Arcila ME, et al. Precision medicine at Memorial Sloan Kettering Cancer Center: clinical next-generation sequencing enabling next-generation targeted therapy trials. *Drug discovery today*. Dec 2015;20(12):1422-1428.
2. Cheng DT, Mitchell TN, Zehir A, et al. Memorial Sloan Kettering-Integrated Mutation Profiling of Actionable Cancer Targets (MSK-IMPACT): A Hybridization Capture-Based Next-Generation Sequencing Clinical Assay for Solid Tumor Molecular Oncology. *The Journal of molecular diagnostics : JMD*. May 2015;17(3):251-264.
3. Schrader KA, Cheng DT, Joseph V, et al. Germline Variants in Targeted Tumor Sequencing Using Matched Normal DNA. *JAMA oncology*. Jan 1 2016;2(1):104-111.
4. Shen R, Seshan V. FACETS: allele-specific copy number and clonal heterogeneity analysis tool for high-throughput DNA sequencing. *Nucleic Acids Res*. 2016;Jun 7:pii:gkw520. Medline:27270079
5. Cancer Genome Atlas N. Comprehensive genomic characterization of head and neck squamous cell carcinomas. *Nature*. Jan 29 2015;517(7536):576-582.
6. Van Loo P, Nordgard SH, Lingjaerde OC, et al. Allele-specific copy number analysis of tumors. *Proceedings of the National Academy of Sciences of the United States of America*. Sep 28 2010;107(39):16910-16915.
7. Morris LG, Riaz N, Desrichard A, et al. Pan-cancer analysis of intratumor heterogeneity as a prognostic determinant of survival. *Oncotarget*. Jan 28 2016.
8. McGranahan N, Favero F, de Bruin EC, Birkbak NJ, Szallasi Z, Swanton C. Clonal status of actionable driver events and the timing of mutational processes in cancer evolution. *Science translational medicine*. Apr 15 2015;7(283):283ra254.
9. Shannon P, Markiel A, Ozier O, et al. Cytoscape: a software environment for integrated models of biomolecular interaction networks. *Genome research*. Nov 2003;13(11):2498-2504.
10. Maere S, Heymans K, Kuiper M. BiNGO: a Cytoscape plugin to assess overrepresentation of gene ontology categories in biological networks. *Bioinformatics*. Aug 15 2005;21(16):3448-3449.
11. Roberts SA, Lawrence MS, Klimczak LJ, et al. An APOBEC cytidine deaminase mutagenesis pattern is widespread in human cancers. *Nature genetics*. Sep 2013;45(9):970-976.
12. Pfeifer GP, You YH, Besaratinia A. Mutations induced by ultraviolet light. *Mutation research*. Apr 1 2005;571(1-2):19-31.
13. Reich M, Liefeld T, Gould J, Lerner J, Tamayo P, Mesirov JP. GenePattern 2.0. *Nature genetics*. May 2006;38(5):500-501.
14. Rifkin R, Mukherjee S, Tamayo P, et al. An Analytical Method for Multiclass Molecular Cancer Classification. *SIAM Review*. 2003;45(4):706-723.
15. Richards S, Aziz N, Bale S, et al. Standards and guidelines for the interpretation of sequence variants: a joint consensus recommendation of the American College of Medical Genetics and Genomics and the Association for Molecular Pathology. *Genetics in medicine : official journal of the American College of Medical Genetics*. May 2015;17(5):405-424.
16. Green RC, Berg JS, Grody WW, et al. ACMG recommendations for reporting of incidental findings in clinical exome and genome sequencing. *Genetics in medicine : official journal of the American College of Medical Genetics*. Jul 2013;15(7):565-574.

eFigure 1.

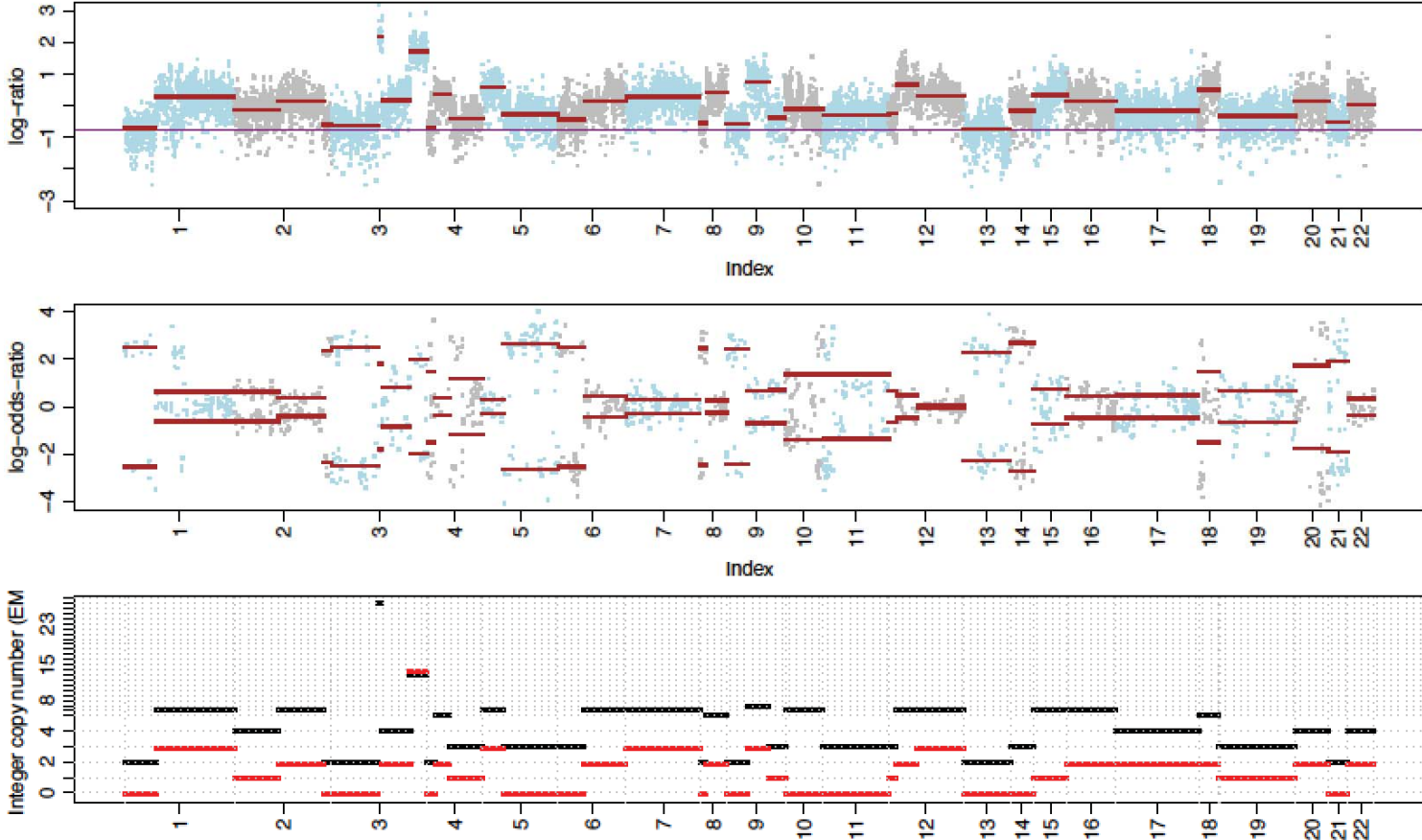
HNSCC tumor with single copy loss of 3p and single copy gain of 3q



eFigure 1. Analysis of whole-genome copy number via targeted capture next-generation sequencing. The MSK-IMPACT platform includes exonic and intronic coverage of selected genes as well as tiling probes across the genome. FACETS is used for segmentation and to determine copy number based on SNP loci read counts. The top plot represents total copy number log-ratio, corrected for library size and GC content. The middle plot represents allelic imbalance (similar to B-allele frequency), using variant allele log-odds ratio, which includes both tumor and normal allelic information. The bottom plot represents allele-specific integer copy number. The case depicted is a tumor (HPV-negative HNSCC) with single copy loss of 3p and single copy gain of 3q.

eFigure 2A.

HNSCC tumor with whole genome duplication and copy-neutral loss of heterozygosity at 3p

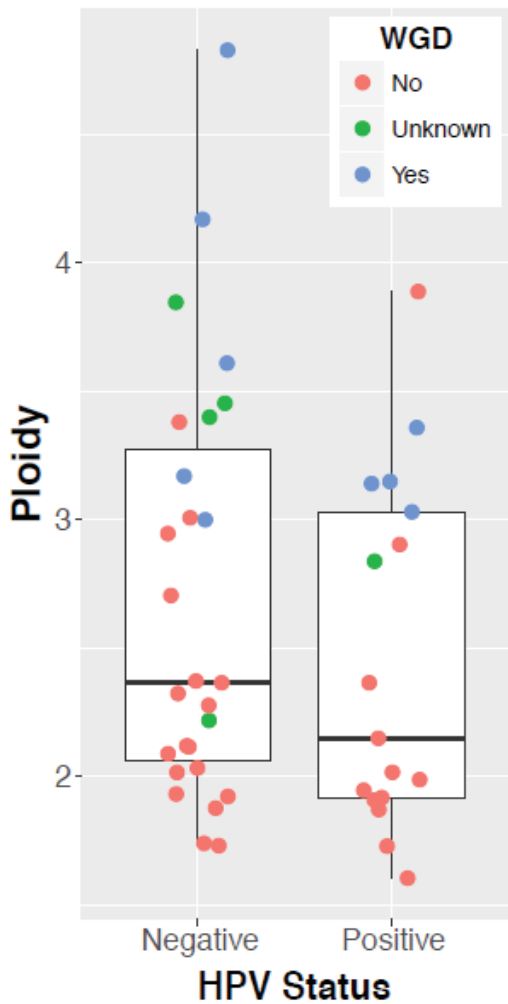


eFigure 2. Analysis of whole-genome copy number via targeted capture next-generation sequencing, as depicted in eFigure 1, showing whole genome duplication. (A) A representative case of a tumor (HPV-negative HNSCC) with whole genome duplication and copy-neutral loss of heterozygosity at 3p. (B) Ploidy in HPV-positive and HPV-negative HNSCC tumors. (C) Whole genome duplication and 3p deletion in HNSCC tumors.



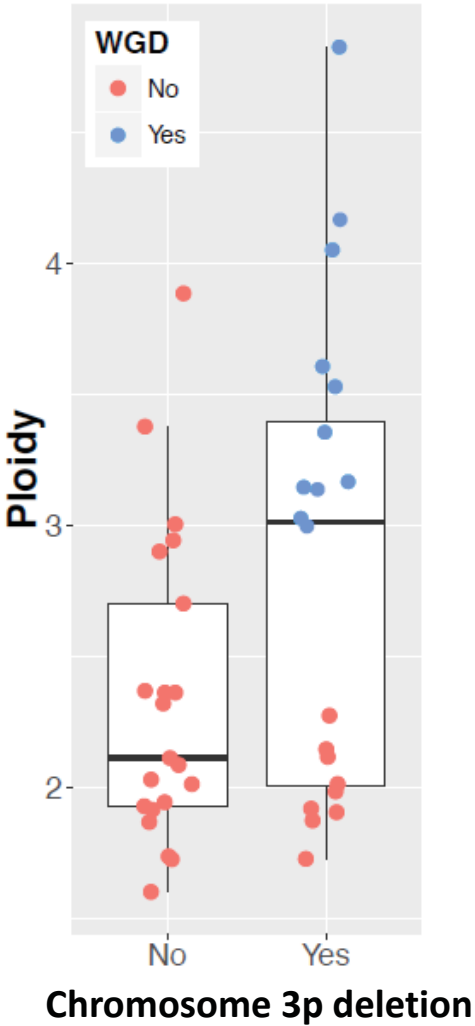
eFigure 2B.

Ploidy and whole-genome duplication (WGD) in HPV-positive and HPV-negative HNSCC tumors

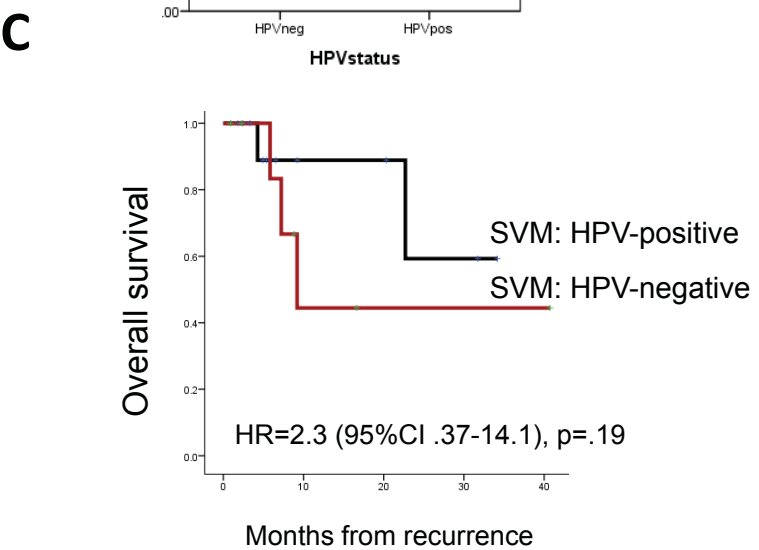
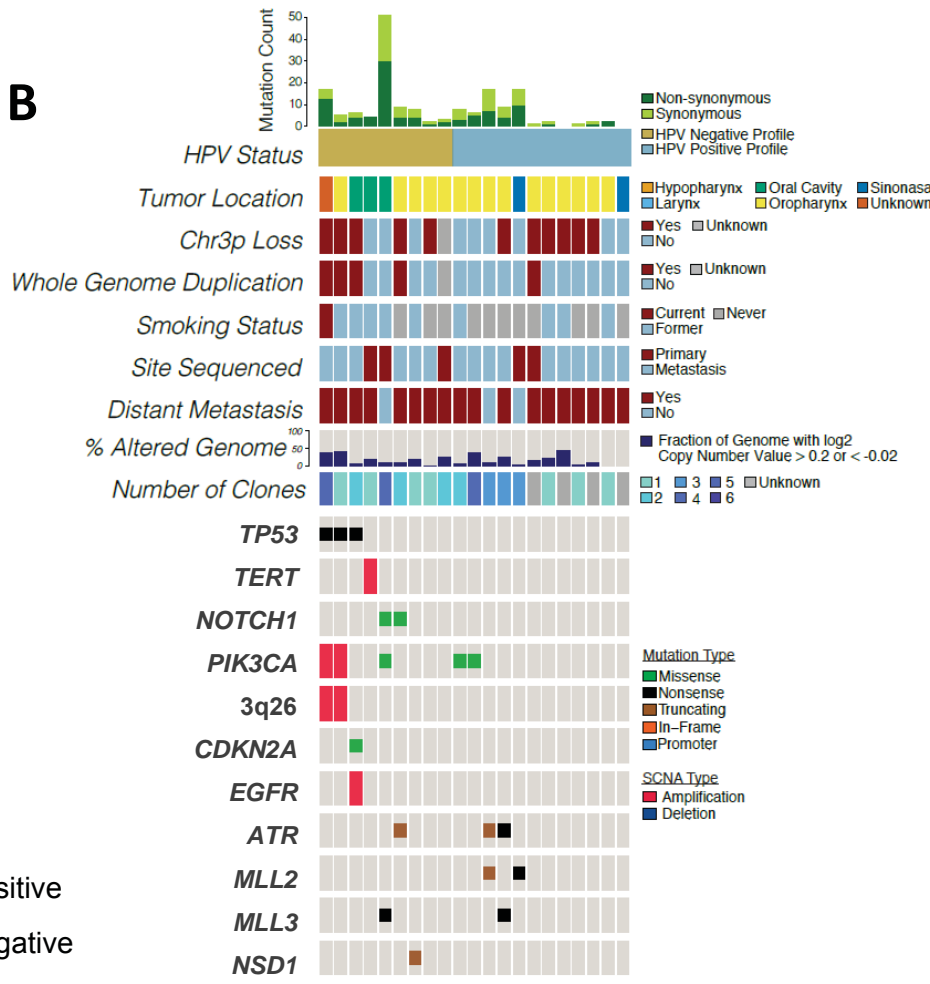
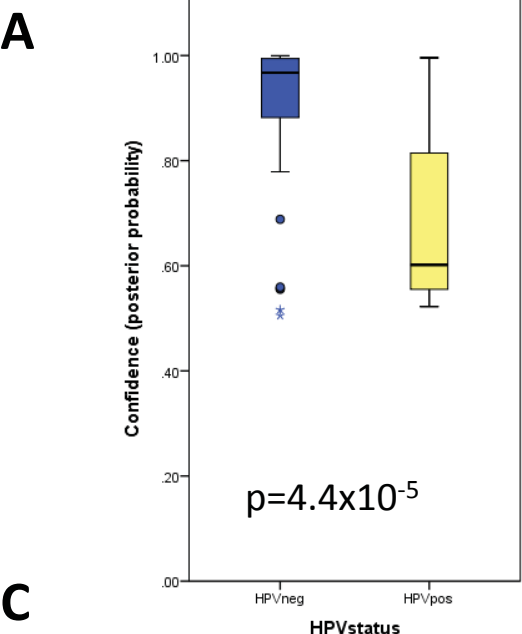


eFigure 2C.

Whole genome duplication (WGD) in 3p-deleted HNSCC tumors  
WGD in 3p-deleted vs. 3p-normal tumors:  $p=.0001$

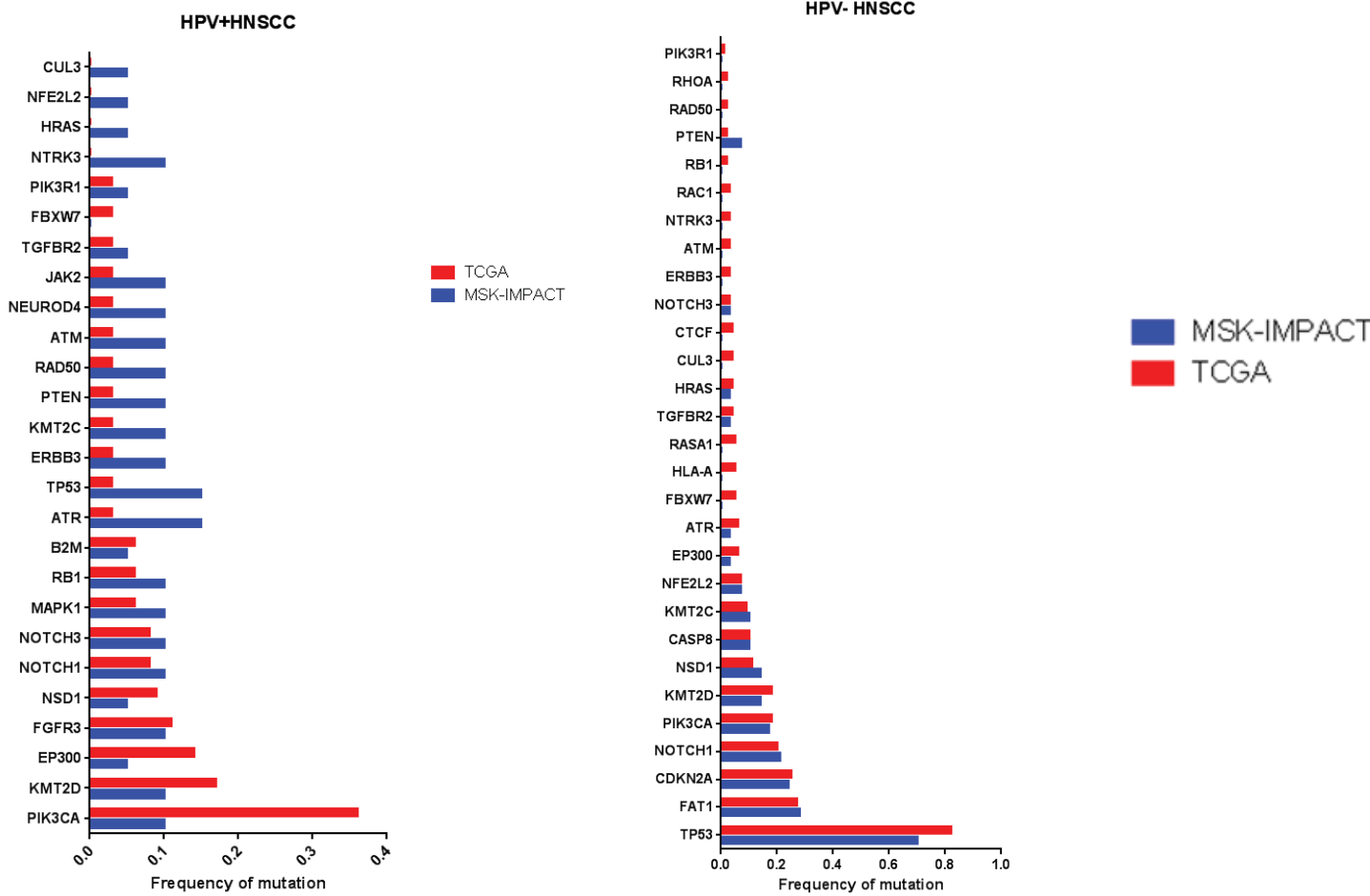


eFigure 3.



eFigure 3. (A) Posterior probabilities of Support Vector Machine (SVM) algorithm, used to classify HPV status based on genetic alterations in MSK-IMPACT HNSCC cases. X-axis reflects actual HPV status. Y-axis reflects the confidence level of the classification, described in Methods. (B) Alterations present in the HPV-positive (MSK-IMPACT) HNSCC cases that were classified as HPV-negative or HPV-positive by SVM. (C) Overall survival of HPV-positive HNSCC cases in MSK-IMPACT cohort, based on SVM categorization as HPV-positive or HPV-negative.

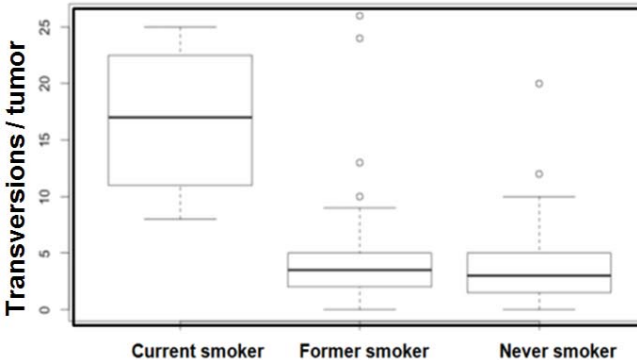
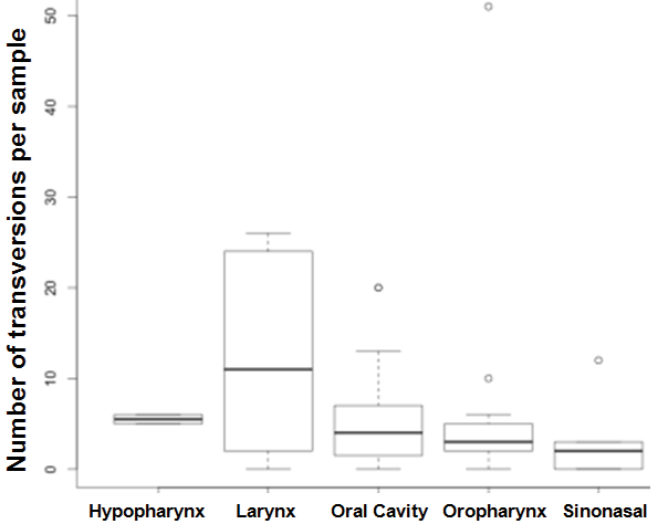
eFigure 4.



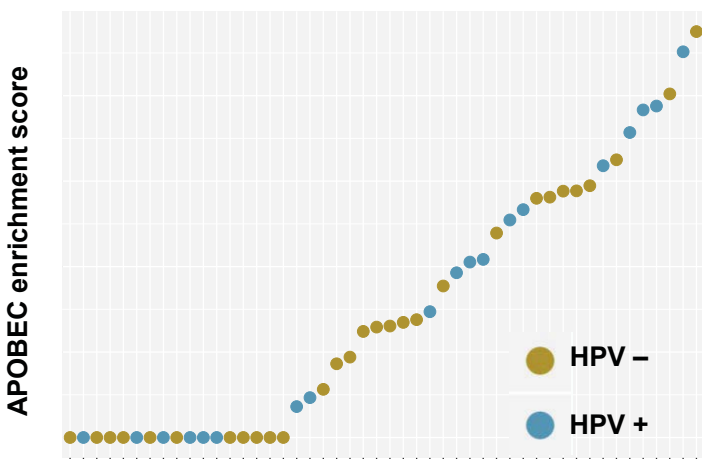
eFigure 4. Comparison of mutational frequencies in recurrent/metastatic HNSCC (MSK-IMPACT) and primary HNSCC (TCGA) tumors, either HPV-positive (left bar graph) or HPV-negative (right bar graph).

eFigure 5.

### Tobacco signature

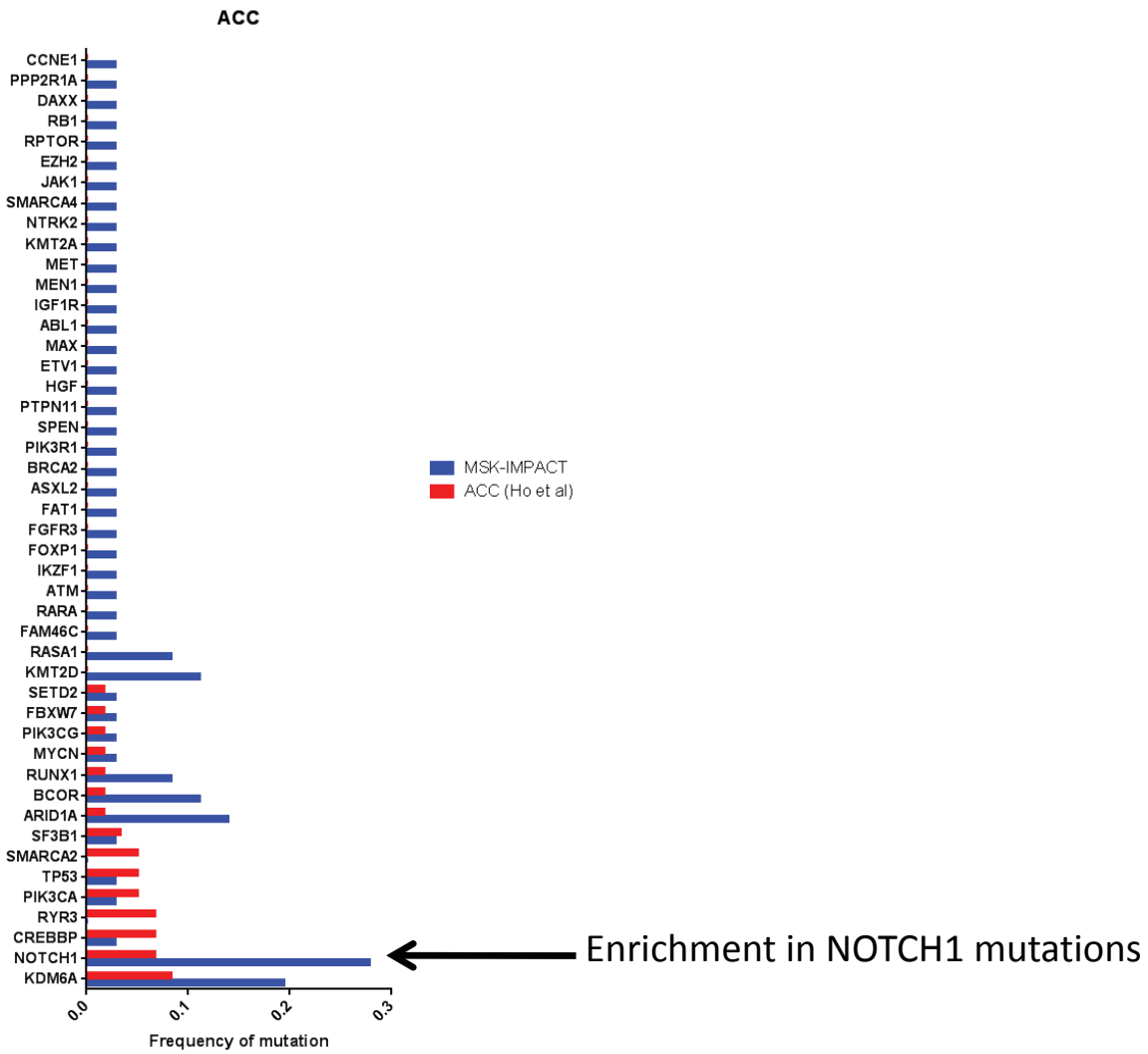


### APOBEC signature



eFigure 5. Distribution of tobacco signature (transversions per tumor) by HNSCC subsite, indicating that transversion-high tumors were mostly laryngeal cancers.

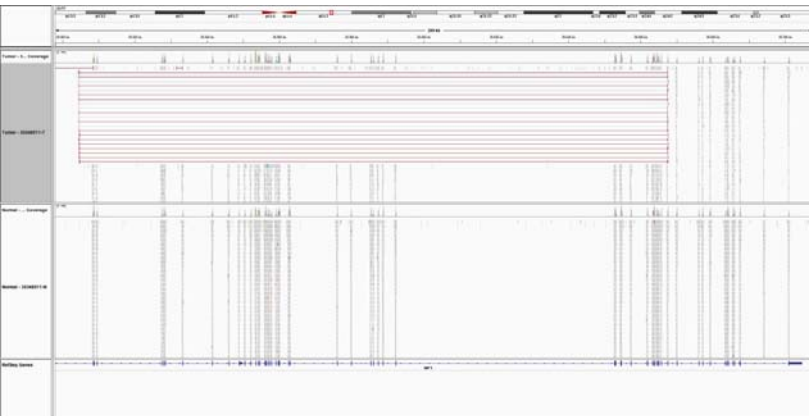
eFigure 6.



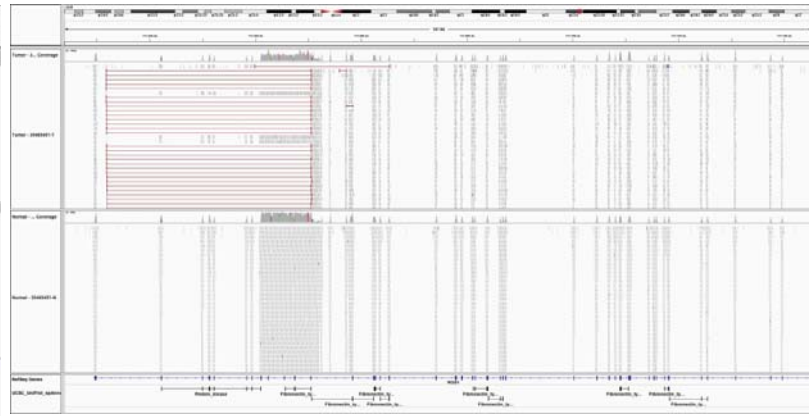
eFigure 6. Comparison of mutational frequencies in recurrent/metastatic ACC (MSK-IMPACT) and primary ACC tumors (Ho et al, Nature Genetics 2013).

eFigure 7.

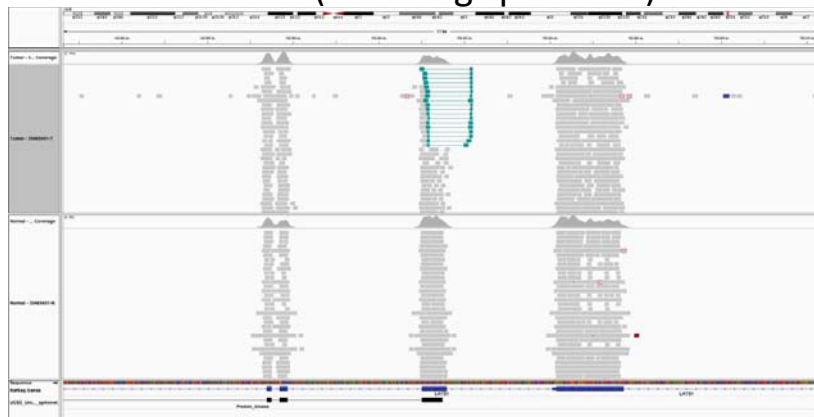
**NF1 intragenic deletion**



**ROS1 intragenic deletion**  
Exons 32-42 (including kinase domain)



**LATS1 intragenic inversion**  
Exon 5 (involving splice site)



eFigure 7. Structural variants observed in salivary duct carcinomas: Integrative Genomics Viewer (IGV) panels.

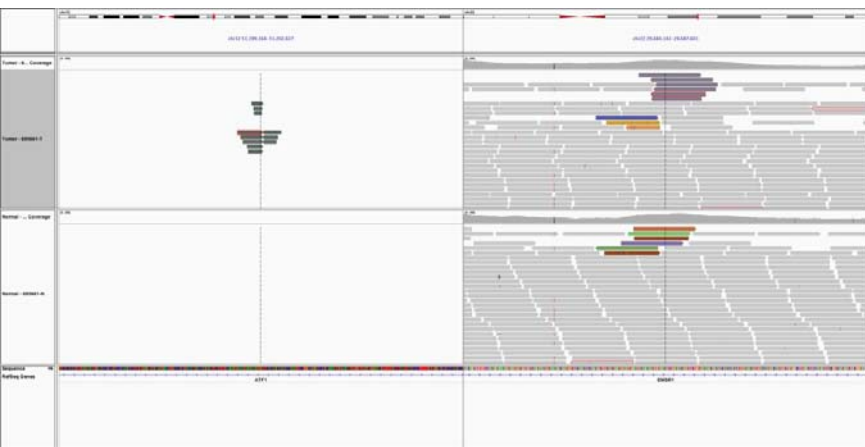
**eFigure 8. ETV6-NTRK3 fusion**



eFigure 8. ETV6-NTRK3 reciprocal fusion in a salivary carcinoma, leading to change in diagnosis to mammary analog secretory carcinoma (MASC) of the salivary gland.



eFigure 9.



***EWSR1-ATF1* reciprocal fusion**  
in a clear cell odontogenic carcinoma

t(22;12)(q12.2;q13.12)



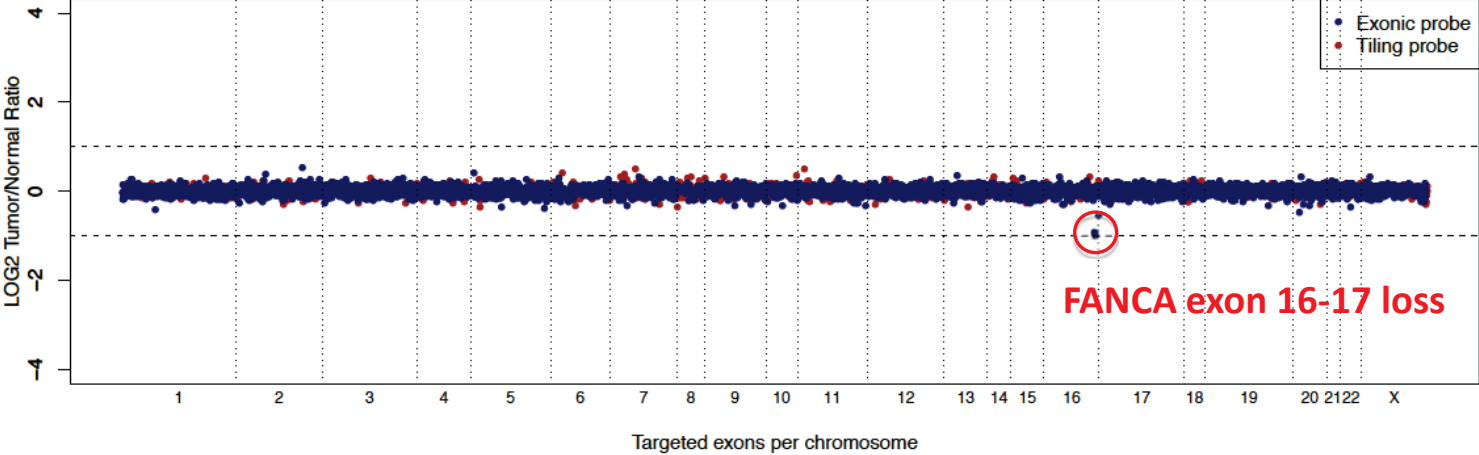
***EWSR1-FLI1* reciprocal fusion**  
in a mandibular cancer initially diagnosed as  
ameloblastic carcinoma, rediagnosed as Ewing  
sarcoma

*EWSR1* exon 7 fused to *FLI1* exon 6  
t(22;11)(q12.2;q24.3)

eFigure 9. EWSR1 fusions in odontogenic carcinomas

eFigure 10.

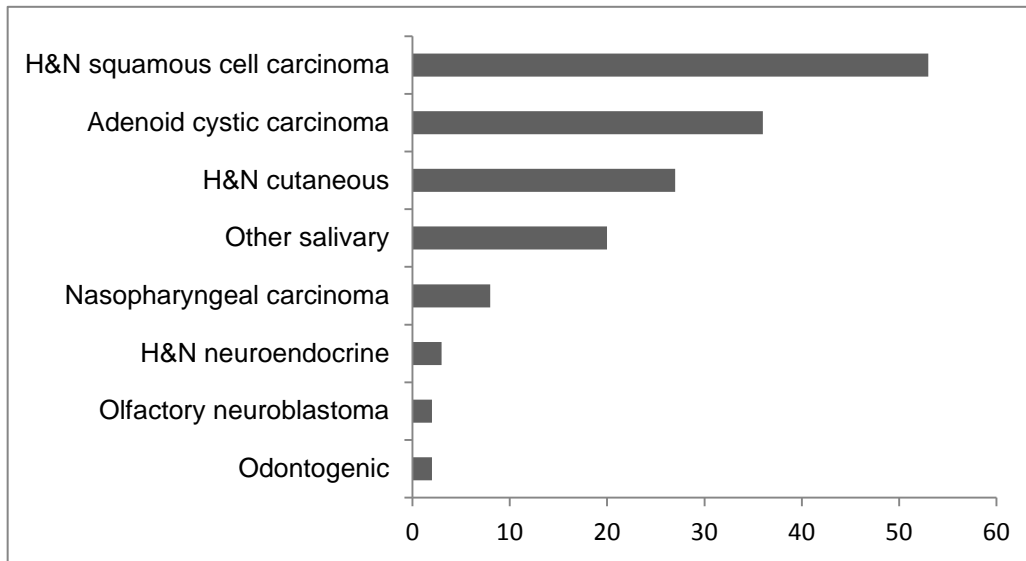
### Germline Copy Number



eFigure 10. Deletion in FANCA observed in germline DNA.

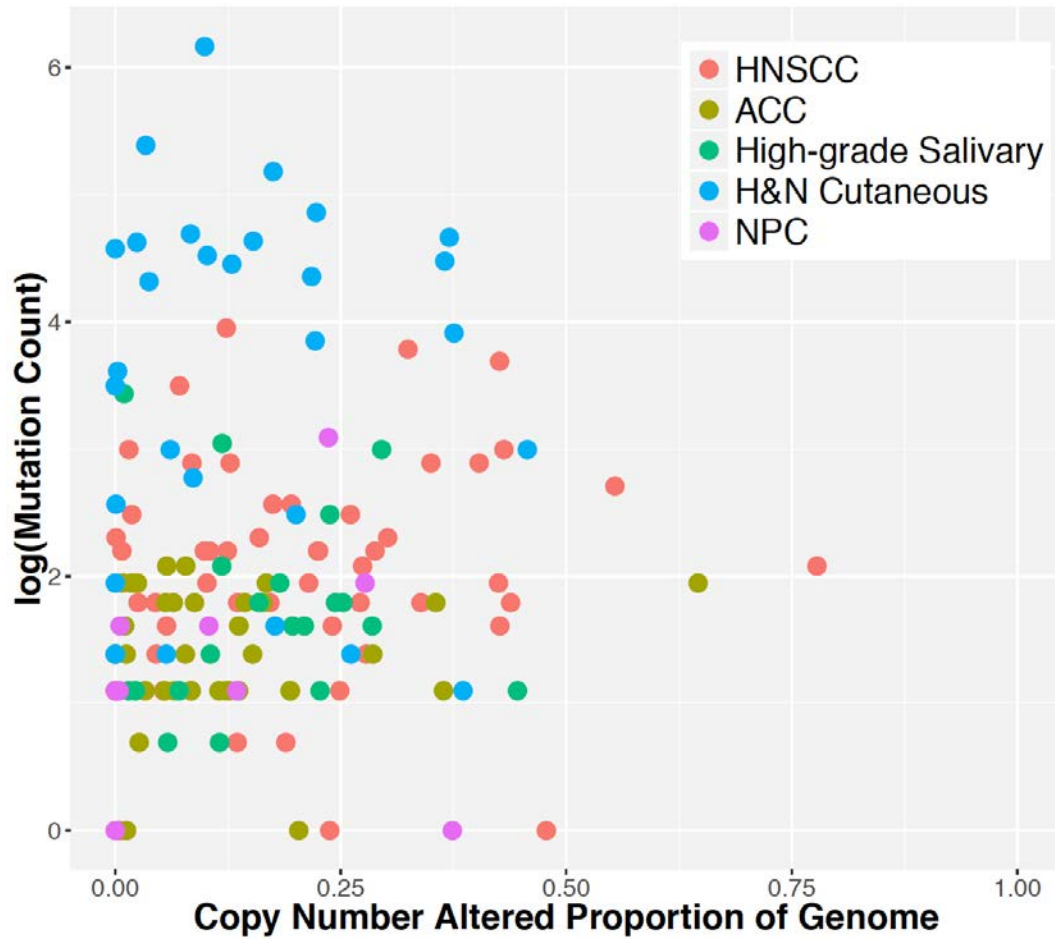
## eFigure 11

Odontogenic	2
Olfactory neuroblastoma	2
H&N neuroendocrine	3
Nasopharyngeal carcinoma	8
Other salivary	20
H&N cutaneous	27
Adenoid cystic carcinoma	36
H&N squamous cell carcinoma	53



eFigure 11. Advanced head and neck cancers profiled using a precision oncology sequencing platform

eFigure 12



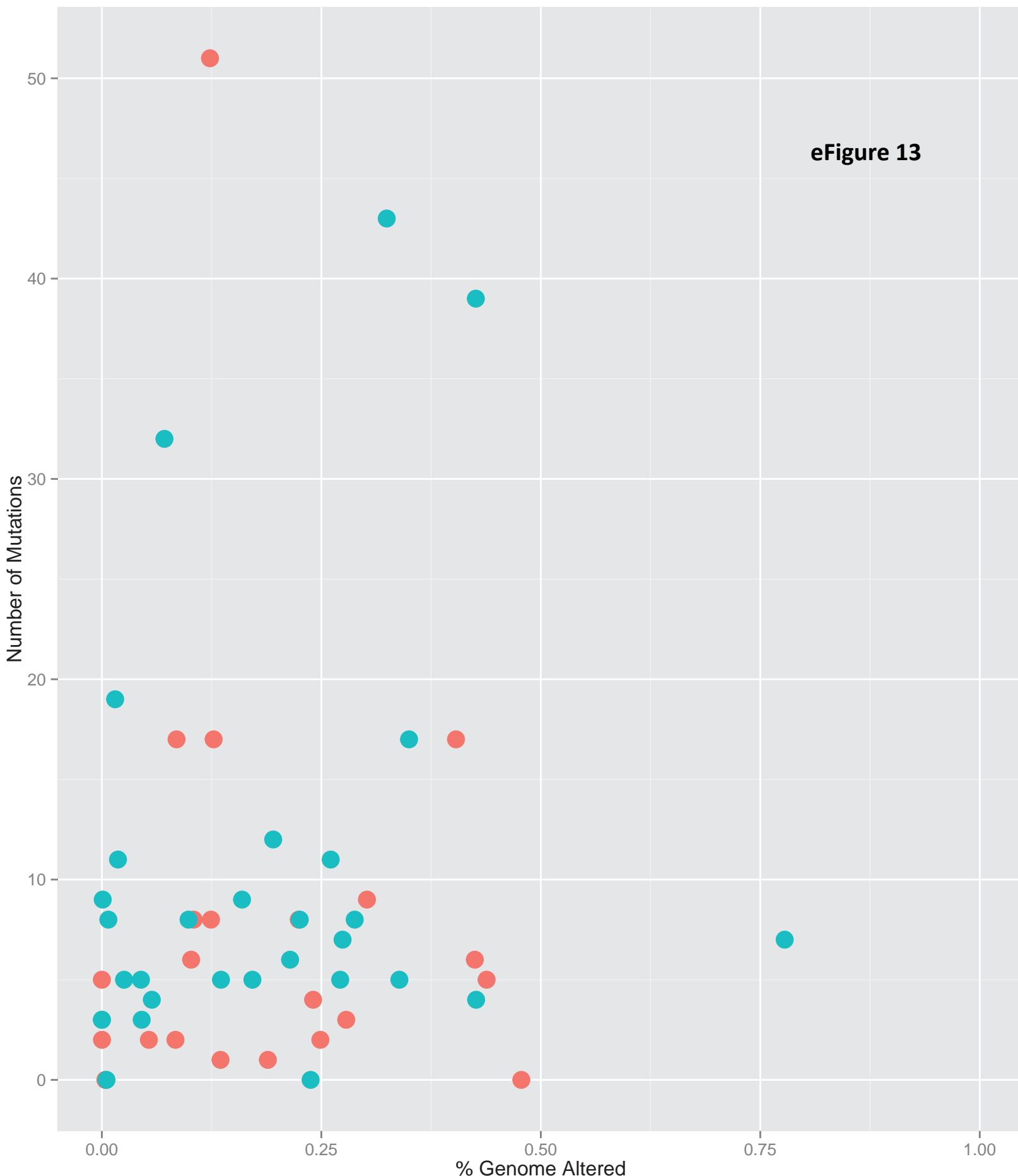
eFigure 12. Scatterplot of log (mutation count) and fraction of genome with copy number alteration, by tumor type

HNSCC, head and neck squamous cell carcinoma. ACC, adenoid cystic carcinoma. NPC, nasopharyngeal carcinoma.

eFigure 13

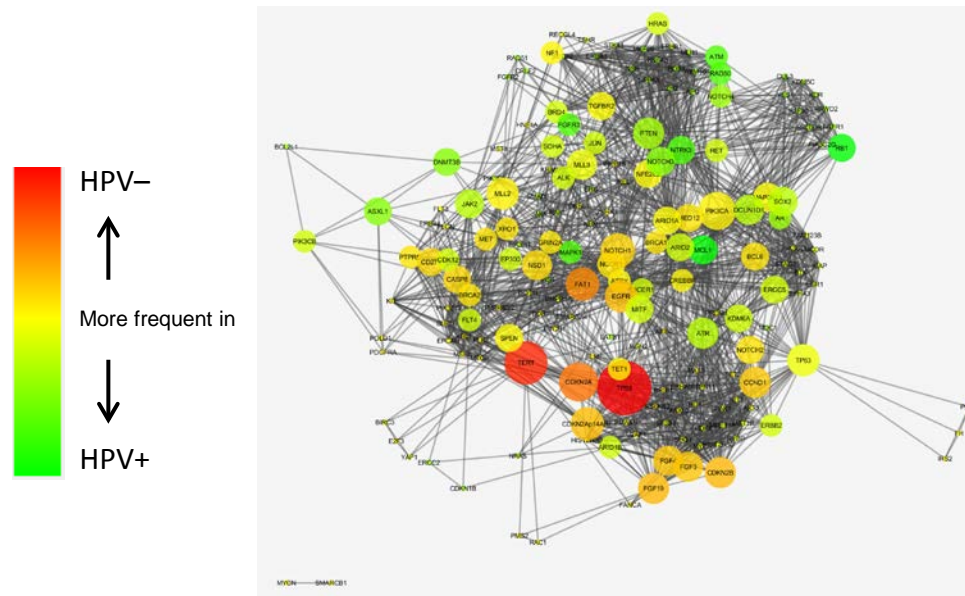
Subgroup

- HPVpos
- HPVneg



eFigure 13. (Above) Scatterplot of mutation counts and percentage of genome with copy number alteration, by human papillomavirus (HPV) status in head and neck squamous cell (HNSCC) samples.

## eFigure 14

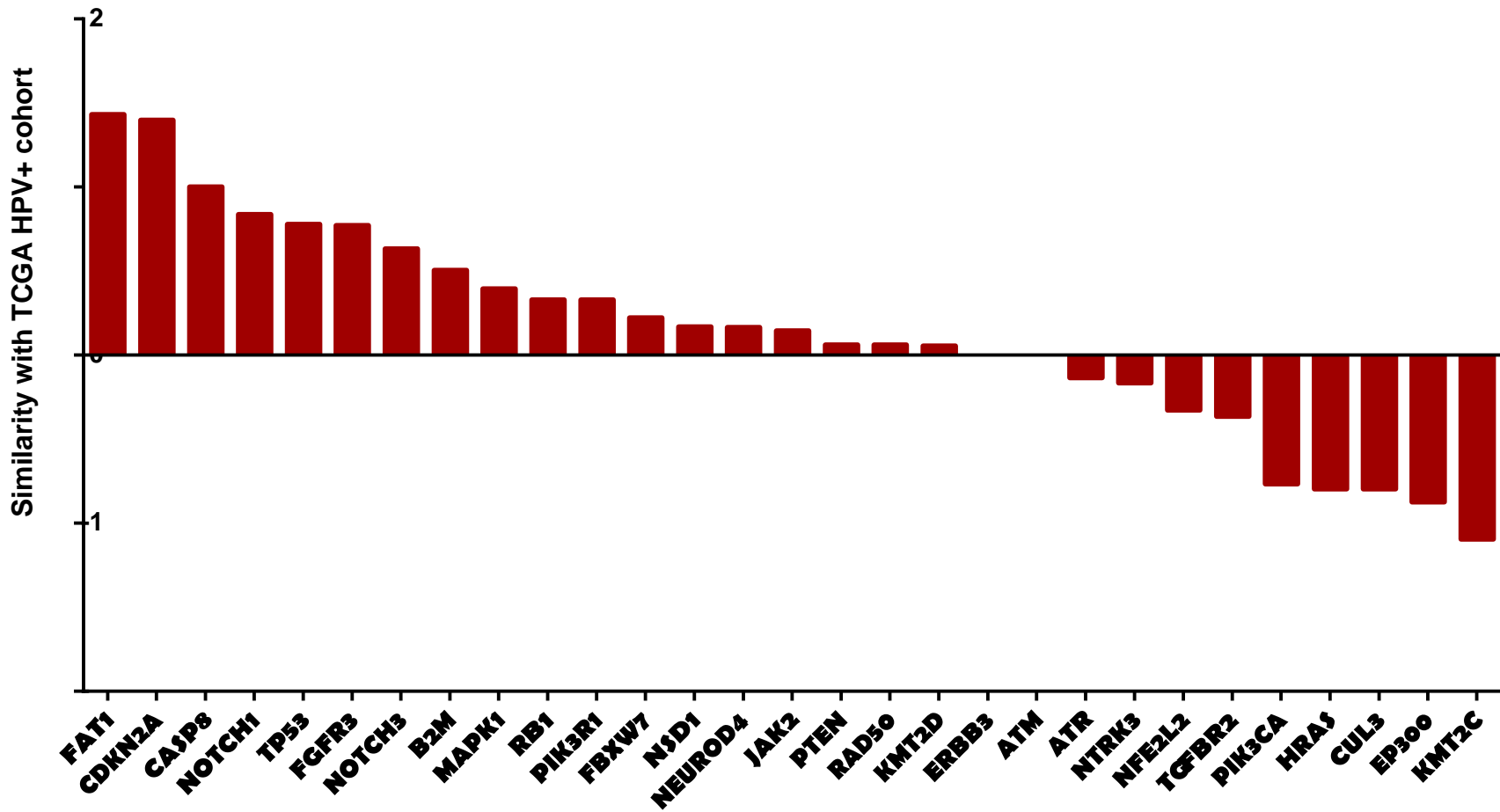


eFigure 14. Correlation network of somatic alterations, where the color of nodes represents relative predominance in HPV-positive or HPV-negative tumors, the size of the nodes represents frequency of alteration, and edges represent correlations or anti-correlations.

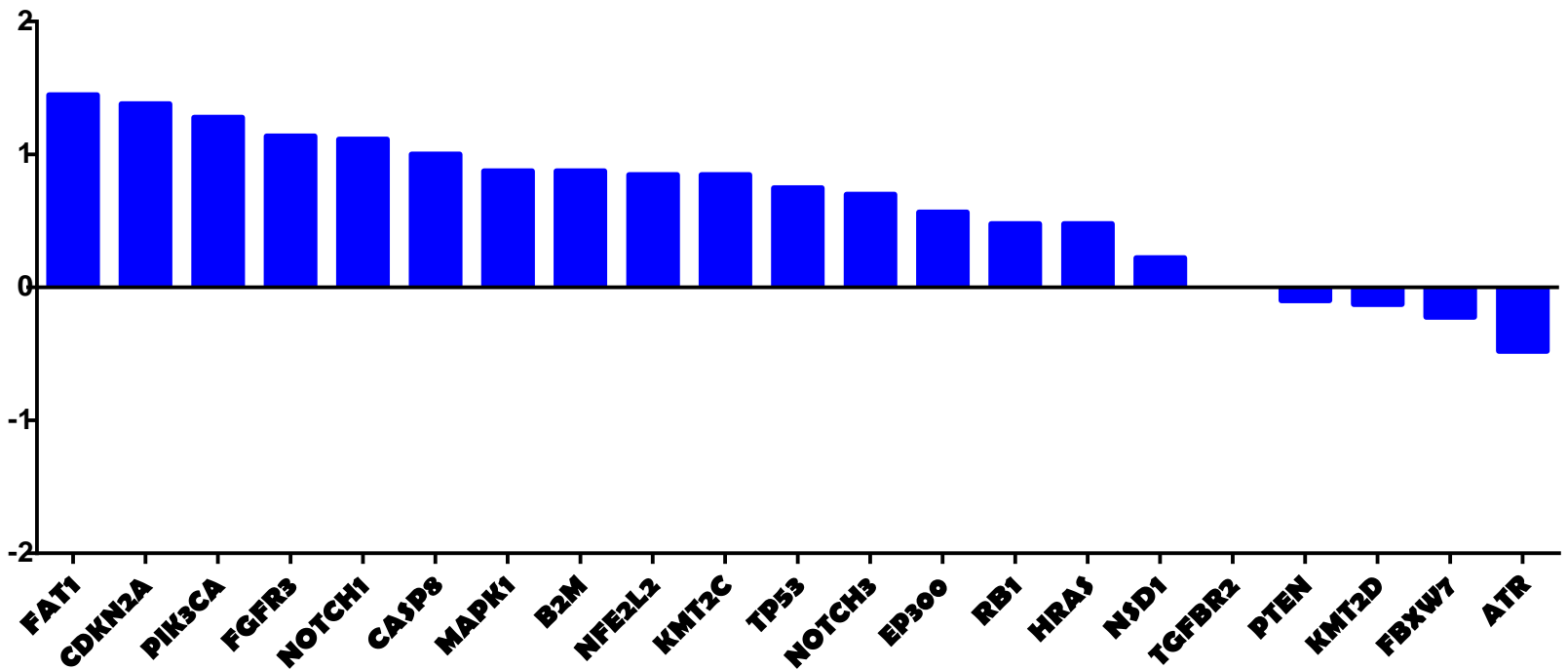




### Similarity of IMPACT (HPV+) to TCGA (HPV+/-)



### Similarity of IMPACT (HPV-) to TCGA (HPV+/-)

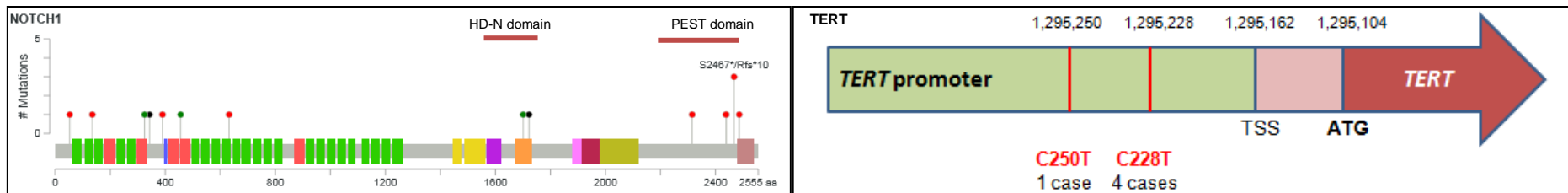


**eFigure 16**

eFigure 16. Column graph representing the most frequent mutations in recurrent/metastatic tumors, and the similarity of mutational frequencies to those in primary HPV-positive/negative tumors. Similarity score is defined as:  $[-\log_{10}(|\text{TCGA}\%_{\text{HPV}\text{same}} - \text{IMPACT}\%|) - \log_{10}(|\text{TCGA}\%_{\text{HPV}\text{different}} - \text{IMPACT}\%|)]$ , for all mutations with average frequency  $>.02$ .

eFigure 17

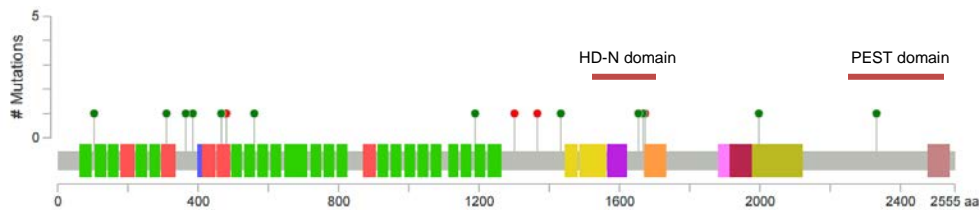
# Adenoid Cystic Carcinoma



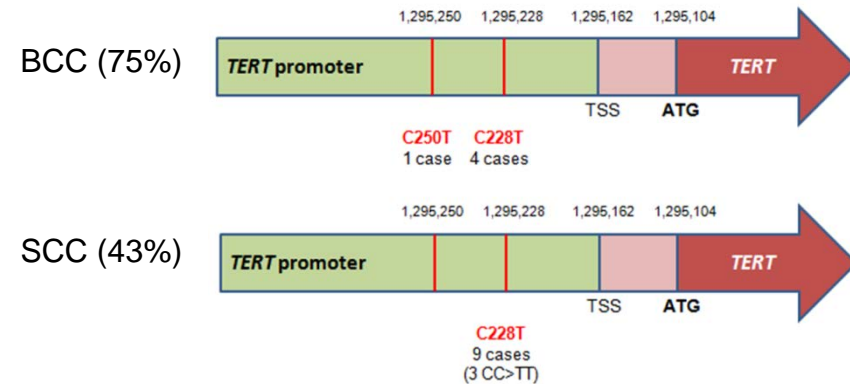
eFigure 17. Mutation Distributions of NOTCH1 and TERT in ACC. Green circles indicate missense mutations; red, truncating; black, inframe insertions or deletions.

## eFigure 18

### NOTCH1 mutations in cutaneous SCC

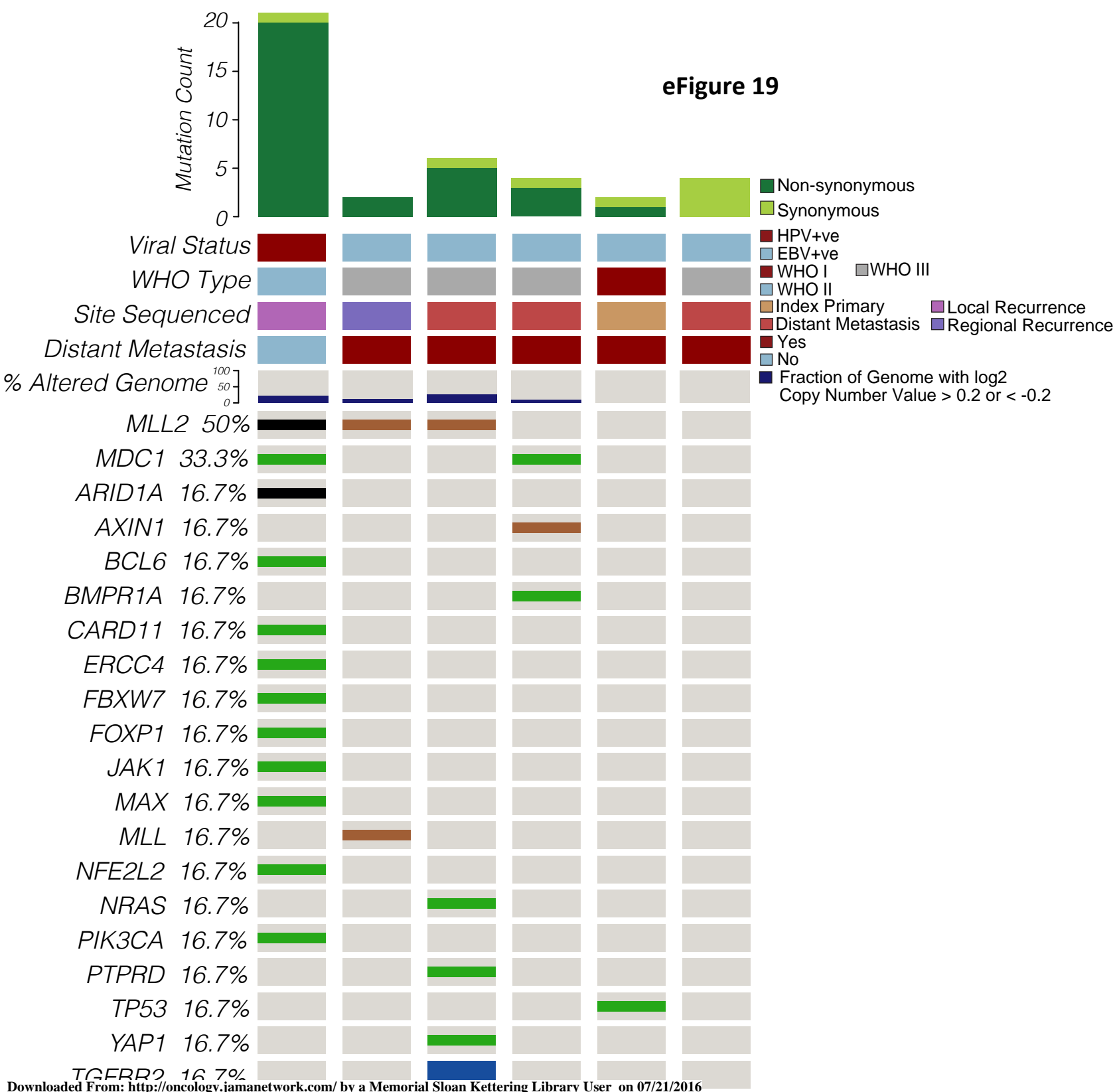


### TERT promoter mutations in cutaneous carcinomas



eFigure 18. NOTCH1 and TERT Mutations in Cutaneous Squamous (SCC) and Basal Cell (BCC) Carcinomas of the Head and Neck. Green circles indicate missense mutations; red, truncating; black, inframe insertions or deletions.

eFigure 19



eFigure 19. (Above) Mutational landscape of recurrent/metastatic nasopharyngeal carcinomas. EBV, Epstein-Barr virus; HPV, Human papillomavirus.